

Coupling carbon nanotube mechanics to a superconducting circuit: Supplementary Information

B.H. Schneider¹, S. Etaki¹, H.S.J. van der Zant¹, G.A. Steele¹

¹*Kavli Institute of NanoScience, Delft University of Technology, PO Box 5046, 2600 GA, Delft, The Netherlands.*

S1 Device characterization

In Fig. S1, we present electrical measurements characterizing the transport properties of the device, in which the Coulomb blockade and Fabry-Perot transport regimes for different gate voltages can be seen, and from which the bandgap is estimated.

S2 Discriminating gate-induced flux from time-dependent flux creep

In this section, we present measurements which discriminate between time dependent magnetic flux creep (Fig. 2c in the main text) and gate-induced flux (Fig. 3b of the main text). This is done by plotting the time-dependent oscillations of I_C at different gate voltages. If the gate is inducing no flux in the SQUID, the oscillations at different gate voltages should all be in phase. If the gate is inducing a flux in the SQUID, there will be a phase shift between the oscillations at different gate voltages.

In Fig. S2, we demonstrate that at $B = 0$, the oscillations in time at different gate voltages are in phase, while $B = 250$ mT, they are shifted by the gate-induced flux. The data in Fig. S2 are extracted from a 3-D $(x, y, z) = (I_B, V_G, t)$ dataset (one at $B = 0$ and one at $B = 250$ mT). The measurements are performed by sweeping the bias current, stepping the gate voltage quickly, and then repeating this in time. The gate sweep is performed quickly enough such that the measurement time for a full gate sweep measurement, as shown in Fig. S2a, is fast compared to the external flux drift: the measurement time for such a gate sweep is $t_{meas} = 7$ min, while the external flux creep rate during these measurements is about $1 \Phi_0$ in two hours. Each gate sweep can therefore be considered to be taken at a fixed external flux. Note that in addition to the slow flux creep, we also sometimes observe sudden jumps in the external

flux, such as can be seen at $t = 4.2$ hours in Fig. S2d. This results in a sudden jump in the phase of the oscillations. The gate induced phase shift, however, can still be tracked both immediately before and after the jump. The gate traces in Fig. S2 and Fig. 3 of the main text are extracted at timesteps where these flux jumps are not present.

Figure S2b shows I_C vs. time for three different gate voltages at $B = 0$. At zero external field, the oscillations of I_C measured at different gate voltages are all in phase, indicating no gate-induced flux. In Fig. S2d, we show I_C oscillations in time at $B = 250$ mT. The d.c. gate voltage now shifts the phase of the oscillations, as can be seen clearly in Fig. S2d. This gate-dependent phase shift demonstrates that the gate-induced sinusoidal modulation of I_C shown in Fig. S2c, and Fig. 3c of the main text, are indeed caused by a gate-voltage induced magnetic flux.

S3 Expected static displacement of the nanotube with gate voltage

When a constant voltage V_G is applied to the gate, the suspended nanotube segments are attracted to the gate by a Coulomb force, $F_C \propto V_G^2$. The equilibrium position of the nanotube corresponds to the position where this Coulomb force is balanced by the mechanical restoring force [1]. At small gate voltages, the bending rigidity of the nanotube dominates the mechanical restoring force, giving a static displacement $u \propto V_G^2$ (the weak bending regime). Beyond a certain gate voltage, induced tension in the nanotube becomes important in determining the mechanical restoring force, and there is a transition to a strong bending regime in which $u \propto V_G^{2/3}$. The transition between these two regimes depends on the dimensions of the nanotube, and can also be influenced by additional tension introduced, for example, by the fabrication process. In any case, the net result is that the displacement of the nanotube as a function of gate voltage is, to a good approximation, linear over a relatively wide regime of voltages, as can be seen in Fig. 2 of Sapmaz *et al.* [1].

If the nanotube displacement was not linear in gate voltage, the periodicity of the I_C oscillations in gate voltage, ΔV_G^{-1} , would change slowly as a function of gate voltage. The relatively constant ΔV_G^{-1} we observe in Fig. 4a of the main text indicates that the nanotube displacement in our device is indeed approximately linear in the range of gate voltages we study.

Critical current oscillations in gate voltage were fitted to a cosine function:

$$f(x) = \frac{a+b}{2} + \frac{a-b}{2} \cos \left[(x-x_0) \frac{2\pi}{L} \right] \quad (1)$$

where a and b are the maximum and minimum of the modulation respectively, and where x_0 is the position at the maximum and L the periodicity.

S4 Definition of the nanotube displacement and estimation of the flux responsivity

In this section, we give a rigorous definition of the nanotube displacement, and use this definition to calculate the flux responsivity of the device. In particular, following Poot *et al.* [2], we define the displacement of a mode of the nanotube in such a way that we require only one effective mass for all modes, avoiding the complication of having different effective masses for different modes.

The zero-frequency, or dc, flexural displacement $z_{\text{dc}}(x, y)$ of the carbon nanotubes towards the back gate (the $x-y$ plane), can be described by a single coordinate u_{dc} . The displacement per unit force and the change of area ΔA per unit displacement both depend on the chosen definition of u_{dc} . This is also true for the mechanical resonance modes of the nanotube, which form an eigenbasis for the nanotube displacement. Any periodic displacement of the nanotube with frequency f can be decomposed into a superposition of the eigenmodes:

$$z(x, y, t) = \sum_0^{\infty} u_n \xi_n(x, y) \cos(2\pi f t + \varphi_n), \quad (2)$$

where u_n is the displacement coordinate, $\xi_n(x, y)$ is the normalized mode shape, f_n is the eigenfrequency and φ_n is the phase offset of mode n . For a nanotube with length ℓ much larger than its cross-sectional diameter, $\xi_n(x, y)$ is usually integrated in the radial direction, such that the mode shape can be described as a function of only the distance along its length direction, x , i.e. $\xi_n(x, y) \rightarrow \xi_n(x)$. The dc displacement ($f = 0$) is related to the eigenmodes by:

$$z_{\text{dc}}(x) = \sum_0^{\infty} u_n \xi_n(x). \quad (3)$$

In general, the displacement, modeshapes and eigenfrequencies of the nanotube must be solved from its elastodynamic differential equations and depend on the nanotube geometry, its rigidity, any built-in tension, and the amount and distribution of applied forces. Once this is done, the definition of

displacement depends on the choice of normalization for $\xi_n(x)$. A convenient normalization for $\xi_n(x)$ is:

$$\frac{1}{\ell} \int_0^\ell \xi_n(x)^2 dx = 1. \quad (4)$$

With this normalization, the displacement coordinate u_n is (spatial) root-mean-square displacement of mode n . The dynamical spring constant of each eigenmode now equals $k_n = m_R(2\pi f_n)^2$, where m_R is the nanotube mass. The change in area due to a d.c. nanotube displacement becomes:

$$\Delta A = \int_0^\ell z_{\text{dc}}(x) dx = \sum_0^\infty a_n \ell u_n, \quad (5)$$

$$a_n \equiv \frac{1}{\ell} \int_0^\ell \xi_n(x) dx. \quad (6)$$

To estimate the numerical coefficients a_n , we assume sinusoidal eigenmode shapes for the nanotubes: $\xi_n(x) = \sqrt{2} \sin(\pi n x / \ell)$ (based on [2]). The numerical coefficients then become $a_n = 0.9/n$ for odd n and $a_n = 0$ for even n (no net area change). For a displacement due to a uniformly distributed dc force, the amplitude of each eigenmode is proportional to $(a_n/f_n)^2$, which means that the shape of the dc deflection is almost entirely determined by the fundamental eigenmode (f_n is roughly proportional to n). The dc spring constant is then equal to k_1 and the area change for both u_{dc} and u_1 is characterized by the same coefficient, $a_1 = 0.9$.

Having defined the displacement, we are now in a position to calculate the responsivity of the device. The flux responsivity Φ_u which we give in the main text is calculated by multiplying ΔA with the applied magnetic field B and dividing out the displacement u_{dc} :

$$\Phi_u \equiv \frac{d\Phi}{du_{\text{dc}}} \approx \frac{d\Phi}{du_1} = a_1 B \ell. \quad (7)$$

At a field of 1 T and a suspended nanotube length of 800 nm, we get a responsivity $\Phi_u = 0.35 \Phi_0/\text{nm}$ per suspended nanotube segment. The dc displacement of the nanotube due to the applied gate voltage can now be calculated based on Fig. 4a of the main text: At 1 T, we observe five oscillations of the SQUID critical current, i.e. $\Delta\Phi = 5\Phi_0$. With the calculated responsivity, the displacement of each nanotube segment over the full gate voltage range is $\Delta\Phi/\Phi_u = 7$ nm.

S4 Estimation of the zero point motion

Quantum mechanical displacement fluctuations are dominant when a mechanical resonator with resonance frequency f_R is cooled to a temperature T such that its thermal energy is far less than the energy of a

single phonon, i.e. $k_{\text{B}}T \ll hf_{\text{R}}$. Here, k_{B} is the Boltzmann constant and h is the Planck constant. In this regime, the resonator has an average phonon occupation which approaches zero, and displacement fluctuations are due to the quantum mechanical ground state energy of the resonator, which equals that of half a phonon. The root-mean-square value of the ground state displacement fluctuations is called the zero-point motion and is given by [2]:

$$u_{\text{zpf}} = \sqrt{\frac{hf_{\text{R}}}{2m_{\text{R}}(2\pi f_{\text{R}})^2}} \quad (8)$$

The maximum power spectral density $S_{uu}(f)$ due to the zero-point motion occurs at the resonance frequency and is related to u_{zpf} according to [2]:

$$S_{uu}^{\text{zpf}}(f_{\text{R}}) = u_{\text{zpf}}^2 \left(\frac{\pi f_{\text{R}}}{2Q}\right)^{-1} = \frac{hQ}{\pi m_{\text{R}}(2\pi f_{\text{R}})^2} \quad (9)$$

where Q is the quality factor of the resonator. In order to measure the zero-point fluctuations, the measurement sensitivity of the detector should be better (lower) than $S_{uu}^{\text{zpf}}(f_{\text{R}})$. The suspended carbon nanotubes in this paper each have a fundamental eigenmode with displacement in the direction of the back gate. Figure S3 shows a measurement of the mechanical response of the fundamental mode of one of the nanotubes to an applied driving force. From the response curve, we find a resonance frequency of 126 MHz and a quality factor $Q = 3 \times 10^4$. The mass of an 800 nm long single-walled carbon nanotube is approximately $m_{\text{R}} = 5 \times 10^{-21}$ kg (and the corresponding spring constant is thus $k = 3 \times 10^{-3}$ N/m). Using this lower bound for Q gives $u_{\text{zpf}} = 3.6$ pm and $\sqrt{S_{uu}^{\text{zpf}}(f_{\text{R}})} = 45$ fm/ $\sqrt{\text{Hz}}$. With the above responsivity, the zero-point fluctuations of a single suspended nanotube segment result in a flux noise in the SQUID of $16 \mu\Phi_0/\sqrt{\text{Hz}}$.

S5 Estimates of coupling for a nanotube transmon qubit

The zero-phonon coupling rate g is given by the shift in the energy levels of the qubit in response to the zero-point fluctuations of the nanotube position [3, 4]. The zero point fluctuations of $u_{\text{zpf}} = 3.6$ pm together with the responsivity of $0.35 \text{ m}\Phi_0/\text{pm}$ gives a corresponding flux shift of $\Phi_{ZPF} = 1.3 \text{ m}\Phi_0$. In the transmon limit, where the charging energy is much smaller than the Josephson energy ($E_C \ll E_J$), the energy splitting of the qubit is given by [5]:

$$E_{01} \approx \sqrt{8E_J E_C} \quad (10)$$

A small change in the qubit energy due to a change in the Josephson energy is then given by:

$$\delta E_{01} = \frac{E_{01}}{2} \frac{\delta E_J}{E_J} \quad (11)$$

We now need to estimate δE_J in response to the Φ_{ZPF} above. Our SQUID shows a near complete suppression of the critical current as a function of flux, allowing us to estimate the change in E_J on the slope of the flux oscillation as

$$\frac{dE_J}{d\Phi} \approx \frac{E_J^{max}}{0.5\Phi_0} \quad (12)$$

The coupling rate g , given by the shift of the qubit energy in response to the zero point fluctuations of the nanotube position, can then be estimated as:

$$g = \delta E_{01}^{ZPF} \approx \frac{E_{01}}{2} \frac{\Phi_{ZPF}}{0.5\Phi_0} \quad (13)$$

Assuming E_{01} is designed to be 6 GHz, and using $\Phi_{ZPF} = 1.3 \text{ m}\Phi_0$, we estimate the coupling to be $g = 7$ MHz.

References

- [1] Sapmaz, S., Blanter, Y., Gurevich, L. & Van Der Zant, H. Carbon nanotubes as nanoelectromechanical systems. *Physical Review B* **67**, 235414 (2003).
- [2] Poot, M. & van der Zant, H. S. Mechanical systems in the quantum regime. *Physics Reports* – (2012).
URL <http://www.sciencedirect.com/science/article/pii/S0370157311003644>.
- [3] LaHaye, M., Suh, J., Echternach, P., Schwab, K. & Roukes, M. Nanomechanical measurements of a superconducting qubit. *Nature* **459**, 960–964 (2009).
- [4] Chan, J. *et al.* Laser cooling of a nanomechanical oscillator into its quantum ground state. *Nature* **478**, 89–92 (2011).
- [5] Koch, J. *et al.* Charge-insensitive qubit design derived from the cooper pair box. *Physical Review A* **76**, 042319 (2007).
- [6] Huttel, A. *et al.* Carbon nanotubes as ultrahigh quality factor mechanical resonators. *Nano Letters* **9**, 2547–2552 (2009).

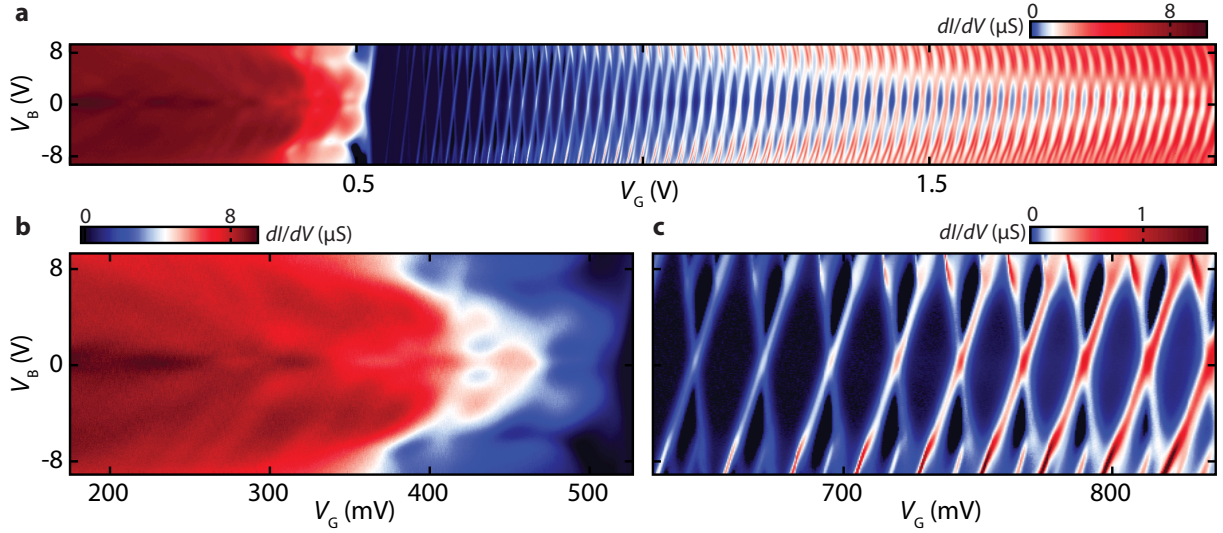


Figure S1: Two-terminal differential conductance **a**, as a function of the source-drain bias voltage V_B and gate voltage V_G , taken at 1.2 K (series resistance from wiring and filters has not been subtracted). This dataset was taken during an earlier cooldown of the device in a different cryogenic insert. As a result, there is a slight shift of the threshold gate voltage for hole conductance compared to Fig. 1c of the main text. We determine the bandgap of the device from the size of the empty Coulomb diamond by subtracting the average of the $1e/1h$ addition energies from the empty-dot addition energy. **b**, Zoom of the dataset showing the high-conductance Fabry-Perot regime when doping the device with holes. **c**, Zoom of dataset showing Coulomb blockade when the device is doped with electrons. When doping the device with electrons, tunnel barriers naturally form from p-n junctions near the edge of the trench. The p-n junctions arise from a gate-independent p-type doping of the nanotube near the trench edge due to the work function difference between the nanotube and the metal contacts.

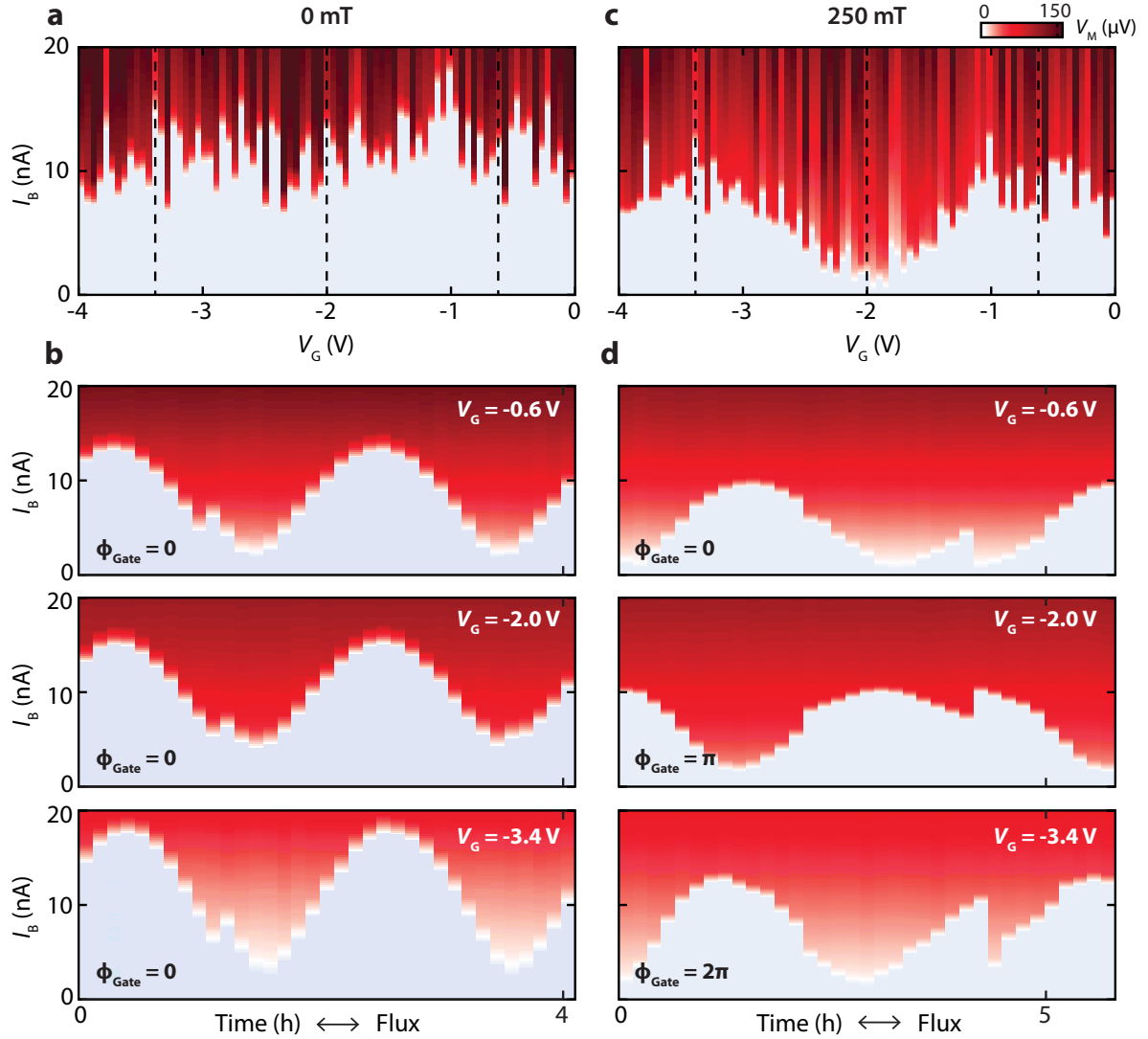


Figure S2: Gate-voltage induced flux observed by a gate-dependent shift of the phase of the time-dependent oscillations of I_C **a**, Voltage V_M as a function of applied bias current I_B and gate voltage V_G at $B = 0$. **b**, V_M as a function of I_B and of time for three different gate voltages indicated by the dashed in **a**. **c,d** Same measurement as in **a,b**, but now taken in the presence of a parallel magnetic field of 250 mT. **d**, A gate dependent phase shift Φ_{Gate} of the oscillations of I_C is now observed, demonstrating that the gate voltage is inducing a magnetic flux in the SQUID.

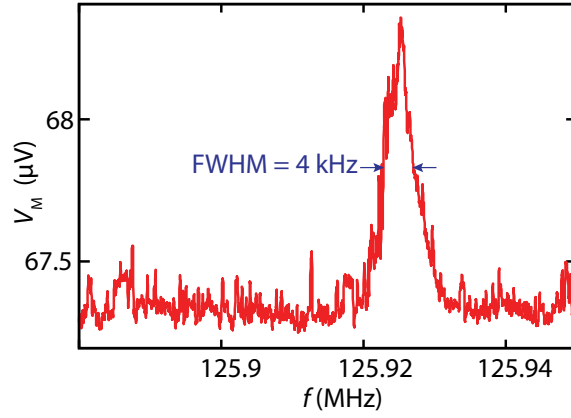


Figure S3: Driven mechanical resonance of the nanotube measured by applying a bias current above the critical current and using rectification readout technique introduced in [6]. We estimate the quality factor of the resonance from the full width at half maximum, Δf , of the measured curve. With $f_R = 126$ MHz and $\Delta f = 4$ kHz, we get $Q = f_R/\Delta f = 3 \times 10^4$.